

# **Dystrophic cardiomyopathy - role of TRPV2 channels in stretch-induced cell damage**

**Charlotte Lorin, Isabelle Vögeli, Ernst Niggli**

Department of Physiology, University of Bern, Bern, Switzerland

Correspondence: Ernst Niggli, Department of Physiology, University of Bern, Buehlplatz 5, 3012 Bern, Switzerland, Phone: +41316318730, Fax: +416314611, E-mail: niggli@pyl.unibe.ch

## Abstract

**Aims**—Duchenne muscular dystrophy (DMD), a degenerative pathology of skeletal muscle, also induces cardiac failure and arrhythmias due to a mutation leading to the lack of the protein dystrophin. In cardiac cells, the subsarcolemmal localization of dystrophin is thought to protect the membrane from mechanical stress. The absence of dystrophin results in an elevated stress-induced  $\text{Ca}^{2+}$  influx due to the inadequate functioning of several proteins, such as stretch-activated channels (SACs). Our aim was to investigate whether transient receptor potential vanilloid channels type 2 (TRPV2) form subunits of the dysregulated SACs in cardiac dystrophy.

**Methods and Results**—We defined the role of TRPV2 channels in the abnormal  $\text{Ca}^{2+}$  influx of cardiomyocytes isolated from dystrophic *mdx* mice, an established animal model for DMD. In dystrophic cells, Western blotting showed that TRPV2 was twofold overexpressed. While normally localized intracellularly, in myocytes from *mdx* mice TRPV2 channels were translocated to the sarcolemma and were prominent along the T-tubules, as indicated by immunocytochemistry. Membrane localization was confirmed by biotinylation assays. Furthermore, in *mdx* myocytes pharmacological modulators suggested an abnormal activity of TRPV2, which has a unique pharmacological profile among TRP channels. Confocal imaging showed that these compounds protected the cells from stress-induced abnormal  $\text{Ca}^{2+}$  signals. The involvement of TRPV2 in these signals was confirmed by specific pore-blocking antibodies and by siRNA ablation of the TRPV2 gene.

**Conclusions**—Together, these results establish the involvement of TRPV2 in a stretch-activated calcium influx pathway in dystrophic cardiomyopathy, contributing to the defective cellular  $\text{Ca}^{2+}$  handling in this disease.

**Keywords:** *mdx* cardiomyocytes, calcium, SACs, TRPV2 channels, dystrophy

## Introduction

Duchenne muscular dystrophy (DMD) is a X-linked degenerative pathology of skeletal muscle, affecting 1 in 3'500 male births. Initially, this progressive disease causes muscle weakness and an impaired mobility requiring a wheelchair by 8-12 years of age. Subsequently, DMD is responsible for the slow development of respiratory failure. Medical advances, such as therapies for respiration support, have prolonged the life expectancy of patients to around 25 years. However, cardiac muscle manifestations are present in essentially all patients by 20 years of age. The heart develops a dilated cardiomyopathy (DCM) resulting in cardiac failure and arrhythmias causing the death of ~20% of all patients.<sup>1</sup>

DMD results from a mutation in the *Dys* gene located on the X chromosome. This genetic alteration is responsible for the absence of the protein dystrophin.<sup>2</sup> Dystrophin is a rod-shaped protein expressed in muscle fibers. In cardiomyocytes, its subsarcolemmal and sarcomeric localization along the T-tubule network is essential to maintain the membrane architecture.<sup>3</sup> Dystrophin is associated with the dystrophin-glycoprotein complex (DGC) which is composed of several transmembrane proteins such as  $\alpha$ -,  $\beta$ - dystroglycans;  $\alpha$ -,  $\beta$ -,  $\gamma$ -,  $\delta$ - sarcoglycans and sarcospan. These proteins provide a mechanical link between the extracellular matrix, *via* laminin binding, and the cytoskeleton, *via* F-actin binding.<sup>4</sup> This molecular bridge is thought to preserve the membrane integrity during mechanical stress.<sup>5</sup> The DGC is also involved in the maintenance of the normal cellular  $\text{Ca}^{2+}$  gradient *via* the regulation of several proteins.<sup>6,7</sup> In general, the absence of dystrophin increases the membrane fragility, either directly or indirectly. This can be determined with a variety of experimental techniques and is often detected as an elevated stress-induced  $\text{Ca}^{2+}$  influx from the extracellular space.<sup>8</sup> Generally, two distinct  $\text{Ca}^{2+}$  influx pathways have been considered, both in skeletal muscle fibers and in cardiomyocytes. 1) Localized microruptures of the sarcolemma result in abnormal stress-induced entry of  $\text{Ca}^{2+}$  (and other ions) into the cells.<sup>9,10</sup> 2) As mentioned above, loss of dystrophin seems to be responsible for the dysregulation of a number of proteins, such as stretch-activated channels (SACs), which constitute an alternative pathway for  $\text{Ca}^{2+}$  entry into myocytes.<sup>11,12</sup> SACs are nonselective cation channels with an increased activity triggered by mechanical stress.<sup>13,14</sup>

At present, the molecular identity of SACs is not known, and most likely there are several types of SACs expressed in skeletal and cardiac muscle. Some of the SACs are thought to contain ion channel proteins from the large family of transient receptor potential (TRP) channels, such as TRPV2 or TRPC1. Since preventing abnormal  $\text{Ca}^{2+}$  influx *via* SACs could be a strategy to ameliorate dystrophy (and other diseases), there is considerable interest in the molecular underpinnings and functioning of these channels

In addition to enlarged  $\text{Ca}^{2+}$  sarcolemmal influx, it has been observed that in dystrophic cardiomyocytes the entire  $\text{Ca}^{2+}$  signaling system, in particular the  $\text{Ca}^{2+}$ -induced  $\text{Ca}^{2+}$  release mechanism, shows an abnormal susceptibility to generate exaggerated  $\text{Ca}^{2+}$  signals, such as  $\text{Ca}^{2+}$  sparks and  $\text{Ca}^{2+}$  waves.<sup>15</sup> This seems to result, at least partly, from post-translational modifications of the SR  $\text{Ca}^{2+}$  release channels (a.k.a. ryanodine receptors, RyRs). As a consequence of all these  $\text{Ca}^{2+}$  signaling disturbances, the resting cytosolic concentration was found to be slightly elevated in dystrophic cardiomyocytes.<sup>13</sup>

In the present study we examined whether the transient receptor potential vanilloid type 2 channels (TRPV2) form part of a stretch-activated channel responsible for the abnormal  $\text{Ca}^{2+}$  influx in dystrophic ventricular cardiomyocytes from *mdx* mice, an established animal model for DMD. The TRPV2 overexpression and specific re-localization to the sarcolemma and along the T-tubule network, highlighted by Western blot analysis and immunocytochemistry, show a mobilization of this protein in dystrophic cardiomyocytes. The combination of relatively unspecific pharmacological interventions with specific functional experiments involving pore-blocking antibodies and siRNA mediated ablation of the protein indicate an abnormal TRPV2 activity in dystrophic cardiomyocytes. Together these results suggest the involvement of TRPV2 as a stretch-activated  $\text{Ca}^{2+}$  influx pathway in dystrophic cardiomyocytes, presumably contributing to the defective cellular  $\text{Ca}^{2+}$  handling in these cells.

## Methods

### Cell isolation

All animal procedures conformed to the Guide for the Care and Use of Laboratory Animals published by the US National Institutes of Health and National Research Council of the National Academy of Sciences (NIH Publication No. 85-23, revised 2011), to the Swiss Animal Protection Law (TSchG), and were carried out with permission by local Swiss authorities (permit BE126/12). C57BL/10 mice (4 months old), in the following referred to as wild-type (WT), and C57BL/10ScScn-*mdx* mice of identical age were provided by Profs. M. Rüegg (University Basel, Switzerland) and U. Rüegg (University Geneva, Switzerland) or purchased from Jackson Laboratory. Animals were euthanized by cervical dislocation, followed by rapid removal and enzymatic dissociation of the cardiac tissue as previously described.<sup>16</sup>

## Immunocytochemistry

Cardiomyocytes were fixed with 4 % paraformaldehyde in PBS for 1 h, permeabilized with 0.5 % Triton X-100 in PBS for 1 h at room temperature. A blocking solution of 4 %, bovine serum albumin (BSA) was applied for 1 h. Cells were incubated overnight at 4 °C in a wet chamber with an anti-TRPV2 antibody against an extracellular epitope (1/100; Alomone ACC-039) and an anti-NCX antibody (1/100; Thermo Scientific MA3-926) diluted in PBS 4 %, BSA and 0.5 % Triton X-100. After washing out in PBS, cells were incubated for 2 h in PBS 4 % BSA and 0.5 % Triton X-100 with secondary antibodies (Alexa Fluor 488-conjugated goat anti-rabbit IgG and Alexa Fluor 568-conjugated donkey anti-mouse IgG; 1/100).

## Experimental solutions

The isotonic superfusion solution contained (in mM): 140 NaCl, 5.4 KCl, 1.8 CaCl<sub>2</sub>, 1.1 MgCl<sub>2</sub>, 5 HEPES, and 10 glucose. The osmolarity was 310 mOsm, and pH 7.3. The hypotonic solution contained (in mM): 70 NaCl, 5.4 KCl, 1.8 CaCl<sub>2</sub>, 1.1 MgCl<sub>2</sub>, 5 HEPES, and 10 glucose, and had an osmolarity of 170 mOsm. SKF96365, tranilast, ruthenium red, ryanodine and thapsigargin were added for at least 30 min before the experiment. The phosphate buffer solution (PBS) contained (in mM): 130 NaCl; 2.07 KCl; 1.5 Na<sub>2</sub>HPO<sub>4</sub>; 8 KH<sub>2</sub>PO<sub>4</sub>; pH was adjusted to 7.4 with NaOH.

Most chemicals were obtained from Sigma. Collagenase (type II) was purchased from Worthington, Di-8ANEPPS and fluo-3-AM from Biotium, tranilast from Cayman, thapsigargin and ryanodine from Alomone, 2-aminoethyl diphenylborinate (2-APB) and ruthenium red (RuR) from Fluka, TRPV2 and TRPC1 antibodies from Alomone (ACC-039 and ACC-032 for TRPV2 and ACC-118 for TRPC1). All experiments were performed at room temperature (20°C).

## Confocal microscopy

Examination of immunolabelled samples and Ca<sup>2+</sup> imaging were performed on an inverted laser-scanning confocal microscope (Olympus FV-1000) with a x60 water immersion objective (NA, 1.2). Cells were loaded with fluo-3-AM (5 μM) for 30 min and excited at 473 nm to record the fluorescence between 490 and 590 nm. Amplitude (F/F<sub>0</sub>) and time-course of Ca<sup>2+</sup> transients were computed using ImageJ and Igor Pro software.

To label T-tubules, ventricular myocytes were incubated with 10 μM di-8-ANEPPS for 30 min.<sup>12</sup> After staining, the images of living cells were acquired with the confocal system.

## Western Blot

Proteins were extracted from isolated ventricular cardiomyocytes using NP40 cell lysis buffer (Invitrogen) supplemented with a protease inhibitor cocktail. Protein extracts were dosed using BCA protein assay kit (Thermo scientific) at 562 nm and then divided into samples and denatured by incubation in Laemmli buffer (Sigma) for 10 min at 95°C. Subsequently, samples were subjected to SDS-PAGE and Western blot analysis. The blots were incubated with anti-TRPV2 against an extracellular epitope (1/200; Alomone ACC-039) and anti-actin (1/1000) antibodies overnight at 4°C and then with horseradish peroxidase-conjugated secondary anti-rabbit and anti-mouse (1/10000, Jackson) antibodies for 1 h at room temperature. Finally, the blots were developed with enhanced chemiluminescent (ECL) substrates for detection of HRP enzymatic activity (Thermo scientific). The apparent molecular weights were estimated according to the position of prestained protein markers (Precision plus protein standards; Bio-Rad).

## Biotinylation

Isolated cardiomyocytes were incubated with biotinylation reagent (Sulfo-NHS-LC-Biotin, APExBIO, 0.5 mg/ml in PBS) at 37°C for 2 h. The biotin reagent was removed and cells were washed twice in cold PBS with 100 mM glycine and twice in cold PBS alone. Then, lysates were prepared and dosed as described above. 100 µg of each samples were incubated with 100 µl of streptavidin agarose resin (Thermo Scientific) for 16 hours at 4°C to capture biotinylated proteins. The beads were pelleted and washed in lysis buffer. Captured proteins were eluted at 60°C for 30 min with Laemmli 2X sample buffer containing 40 mg/mL of dithiothreitol. Then they were analyzed by Western blot as described above with primary antibodies: anti-TRPV2 against an extracellular epitope (Alomone ACC-039, 1/100), anti-GAPDH (positive control, Fitzgerald, 1/3000), anti-P44/P42 MAPK (negative control, Cell Signaling, 1/2000).

## Cardiomyocyte culture and transfection

Isolated cardiomyocytes were cultured in Dulbecco's modified Eagle's medium (DMEM) supplemented with insulin (10 mg/mL), HEPES (10 mM), NaHCO<sub>3</sub> (4 mM), blebbistatin (25 µM), cytochalasin D (0.5 µM). TRPV2 siRNA and non-targeting siRNA were obtained from Origene. Transfection of siRNA was performed using GeneSilencer (Genlantis) for 4 h.

Subsequently, this medium was replaced by solution without transfection reagent for 20 h. Lysates were prepared and dosed as described above.

## Real-time Polymerase Chain Reaction

Total RNA from siRNA against TRPV2 and scrambled siRNA dystrophic cardiomyocytes were extracted using RNA purification kit (NucleoSpin RNA, Macherey-Nagel). Mm\_Trpv2\_1\_SG, Mm\_Actb\_1\_SG were used as specific mouse RT-PCR primers (Qiagen). The ACTB housekeeping gene (against  $\beta$ -actin) and TRPV2 gene were amplified in parallel. Real-time RT-PCR was performed using 9 ng/ $\mu$ l of RNA (KAPA SYBR FAST One-Step Universal Kit) and 200 nM of each primer in a total reaction volume of 15  $\mu$ l. Data were recorded on an Eco Real-Time PCR system (Illumina Labgene Scientific SA) and cycle threshold (Ct) values for each reaction were determined using analytical software from the same manufacturer. Each cDNA was amplified in duplicate, and Ct values were averaged for each duplicate. The average Ct value for ACTB was subtracted from the average Ct value for the gene of interest. As amplification efficiencies of TRPV2 genes and ACTB were comparable, the relation  $2^{-\Delta Ct}$  gave the amount of mRNA, normalized by ACTB.

## Statistical analysis

All results are expressed as mean  $\pm$  SEM of n observations. Sets of data were compared using Student's t test, and significance is denoted as \*P<0.05, \*\*P<0.01. N refers to number of animals, n to number of cells.

## Results

### Osmotic stress induces abnormal Ca<sup>2+</sup> signals in dystrophic cardiomyocytes

As reported before, dystrophic muscle cells exhibit an abnormal membrane fragility and increased stretch sensitivity.<sup>5,17</sup> We applied mild osmotic shocks to WT and dystrophic cardiomyocytes mimicking features of mechanical membrane stress during contractions (cell swelling by 15.8% in both, WT and *mdx* myocytes).<sup>15</sup> After 30 minutes loading with the fluorescent Ca<sup>2+</sup> indicator fluo-3-AM, myocytes were briefly superfused with a mildly hypotonic solution (40 s). The fluorescence was recorded to measure Ca<sup>2+</sup> signals before, during and after

the osmotic stress, visible as a transient decrease of fluorescence due to dye dilution (*Figure 1A* and *1B*). As described in previous studies,<sup>15</sup> cardiomyocytes from *mdx* mice displayed an increased fluorescence starting after a mild osmotic stress (*Figure 1B*). For quantitative analysis, we averaged the normalized fluorescence during a 40 s time window after the osmotic stress (*Figure 1C* left). While in WT cells the fluo-3 signal returned to baseline after the stress ( $F/F_0$ :  $0.98 \pm 0.02$ ,  $n=10$ ), the  $Ca^{2+}$ -related fluorescence observed in *mdx* cardiomyocytes was 1.4-fold larger ( $F/F_0$ :  $1.41 \pm 0.09$ ,  $n=13$ ). Besides an abnormally large transsarcolemmal  $Ca^{2+}$  influx, a different extent of  $Ca^{2+}$  loading of the sarcoplasmic reticulum (SR) and/or an elevated sensitivity of the SR  $Ca^{2+}$  release mechanism could explain these increased  $Ca^{2+}$  signals, similar to other pathologies with altered SR function.<sup>16,18</sup> However, applying rapid puffs of caffeine containing solutions to estimate the  $Ca^{2+}$  SR content before and after the osmotic shock did not reveal a difference between dystrophic and WT cells (*Figure 1C* right). But the *mdx* cells lost significantly more  $Ca^{2+}$  than the WT myocytes, as one would expect because of their exaggerated  $Ca^{2+}$  signals. As it has been reported before, the excessive cytosolic  $Ca^{2+}$  signals in *mdx* cardiomyocytes observed here are triggered, at least partly, by  $Ca^{2+}$  influx via several pathways such as local microruptures in the sarcolemma and the abnormal activation of stretch-activated channels (SACs).<sup>9,12,19</sup> The molecular identity of SACs is not yet established, but for quite some time TRP channels have been suspected to play a role.<sup>19</sup> Recently, transient receptor potential vanilloid type 2 (TRPV2) channels have been proposed to be part of these SACs in dystrophic skeletal muscle fibers.<sup>17,20</sup> Therefore, we next carried out experiments to define the role of TRPV2 channels in the abnormal stress induced  $Ca^{2+}$  signals in dystrophic cardiomyocytes.

## **Sarcolemmal TRPV2 localization and overexpression in *mdx* cardiomyocytes**

In cultured dystrophic skeletal muscle myotubes, TRPV2 channels were found to be localized to the sarcolemma, where they mediated abnormal  $Ca^{2+}$  influx from the extracellular space.<sup>7,17</sup> In physiological conditions, TRPV2 channels are mainly localized to intracellular membrane structures, but are known to translocate to the plasma membrane upon specific stimulation, such as by insulin growth factor-1 (IGF-1). Once activated, they participate in the function and structure of cardiomyocytes.<sup>21,22</sup> Therefore, we compared the TRPV2 expression and its subcellular distribution in freshly isolated WT and *mdx* cardiomyocytes (*Figure 2*). Comparative TRPV2 immunocytochemistry in WT cardiomyocytes showed only a staining within the cell (*Figure 2A* left above). In contrast, in *mdx* cells TRPV2 immunofluorescence displayed a strong localization at the sarcolemma and along the T-tubular network (*Figure 2A* left below). This specific localization was confirmed by a double staining against the  $Na^+$ - $Ca^{2+}$



exchanger (NCX) known to be expressed in the plasma membrane (*Figure 2A* middle and left).<sup>23</sup> Western blot analysis indicated a 2-fold TRPV2 overexpression in dystrophic myocytes (*Figure 2B*). The specific membrane bound fraction of TRPV2 was determined using a biotinylation assay, and normalized to GAPDH. The amount of TRPV2 at the plasma membrane was increased 1.6-fold compared to WT cells (*Figure 2C*).

## Functional characterization of sarcolemmal TRPV2 channels

To assess the functional consequences of the membrane specific TRPV2 overexpression in *mdx* cardiomyocytes, we initially used pharmacological tools. TRP channel pharmacology is notoriously unspecific, but the TRPV2 channels have a peculiar pharmacological profile that sets them apart from many other TRP channels. Contrary to most TRP channels, they are not blocked by 2-APB, but become activated (albeit at a high 2-APB concentration of 500  $\mu\text{M}$ ). They are also activated by the organic anion transporter inhibitor probenecid (Pro, 1 mM). Ruthenium red (RuR, 40  $\mu\text{M}$ ) is an unspecific and tranilast (Tran, 1 mM) a somewhat more specific inhibitor of TRPV2 channel activity.<sup>24-26</sup> In order to experimentally examine  $\text{Ca}^{2+}$  influx without interference from SR  $\text{Ca}^{2+}$  release, *mdx* myocytes were preincubated with thapsigargin (Tg, 1  $\mu\text{M}$ ) and ryanodine (Rya, 10  $\mu\text{M}$ ) (*Figure 3A* and *3B*). Subsequently, and prior to the actual experiment, several stimulations with caffeine (Caff, 10 mM) were applied to completely empty the SR. Both, 2-APB and probenecid perfusions induced a  $\text{Ca}^{2+}$  influx upon their application ( $F/F_0$  of  $1.39 \pm 0.05$  and  $1.78 \pm 0.1$ , respectively) (*Figure 3A* and *3B*). This  $\text{Ca}^{2+}$  influx was substantially reduced in the presence of the TRPV2 inhibitors ( $F/F_0$  of  $1.07 \pm 0.01$  for RuR and  $1.28 \pm 0.05$  in the presence of Tran). Taken together, these findings suggest that in isolated cardiomyocytes TRPV2 channels indeed mediate  $\text{Ca}^{2+}$  influx that can be reduced by TRPV2 inhibitors. With its localization in the sarcolemma of dystrophic myocytes and its known activation by hypotonicity and stretch-induced mechanical stimulation,<sup>7,27</sup> a participation of TRPV2 in the excessive cytosolic  $\text{Ca}^{2+}$  signals could be expected.

## Osmotic stress activates TRPV2 channels

To determine whether TRPV2 channels form part of SACs in dystrophic cardiac cells, *mdx* myocytes were exposed to stress in the presence of the TRPV2 inhibitor SKF96365 (*Figure 3C*, left). Data obtained in WT and *mdx* myocytes is replotted from *Figure 1*, for easier comparison. *Figure 3C* indicates that after the stress the  $\text{Ca}^{2+}$ -related fluorescence was 1.6-fold smaller in the presence of 30  $\mu\text{M}$  SKF96365 ( $F/F_{0\text{SKF}}$ :  $0.93 \pm 0.02$  compared to untreated *mdx* cells,  $1.41 \pm$

0.09). In additional experiments we applied the two TRPV2 inhibitors tranilast and RuR during the osmotic stress (*Figure 3D*). The  $\text{Ca}^{2+}$  signal was 1.5-fold smaller in the presence of tranilast, and 1.6-fold in RuR ( $F/F_{0\text{Tran}}$ :  $0.90 \pm 0.01$  and  $F/F_{0\text{RuR}}$ :  $0.93 \pm 0.01$  compared to untreated *mdx* cells,  $1.41 \pm 0.09$ ). These findings are consistent with an involvement of TRPV2 channels. However, at present the TRPV2 pharmacology is not at all specific, as mentioned above.

To allow more specific conclusions regarding the role of TRPV2 channels and their identification as subunits of SACs we used a two-pronged approach: 1) block of the channel pore with antibodies and 2) ablation of TRPV2 with specific siRNA. First, to achieve specific inhibition of TRPV2 channels, *mdx* cardiomyocytes were incubated during 24 h with TRPV2 antibodies raised against an extracellular epitope, thereby blocking the pore to prevent cation influx (*Figure 4A*).<sup>28</sup> Cardiomyocytes kept in short term culture undergo substantial dedifferentiation, even after 24 h. The ends of cardiomyocytes round up and, most important for  $\text{Ca}^{2+}$  signaling, the T-tubular organisation decreases. To slow down this process we added a low concentration of cytochalasin D (0.5  $\mu\text{M}$ ) that protects cardiomyocytes from the detubulation.<sup>29</sup> Compared to untreated *mdx* myocytes, the  $\text{Ca}^{2+}$ -related fluorescence response was 1.4-fold smaller in cells treated with this antibody ( $F/F_0$ :  $0.88 \pm 0.03$ ; *Figure 4B*). As negative control experiments, we incubated cells with antibodies against an intracellular epitope of TRPV2 and against TRPC1 (extracellular epitope). These antibodies did not protect the treated *mdx* cells from increased  $\text{Ca}^{2+}$  signals ( $F/F_0$ :  $1.23 \pm 0.09$ , *mdx* cells;  $1.25 \pm 0.07$ , anti-TRPC1;  $1.09 \pm 0.09$ , anti-TRPV2 intracellular epitope). The SR  $\text{Ca}^{2+}$  content was not different between the various treatment groups excluding a possible modification of the cells caused by the short-term cell culture.

Another strategy to specifically remove the function of a particular protein is to interfere with its expression using siRNA (*Figure 5*). To this end, *mdx* cardiomyocytes were incubated 4 h with siRNA directed against TRPV2 and maintained in culture during 24 h.<sup>30</sup> Transfected *mdx* cardiomyocytes were exposed to osmotic stress (*Figure 5A*).  $\text{Ca}^{2+}$ -related fluorescence was 1.3-fold smaller in cells loaded with TRPV2 siRNA ( $F/F_0$ :  $0.94 \pm 0.02$ ) compared to the negative control ( $F/F_0$ :  $1.27 \pm 0.09$ , *Figure 5B*). No difference was observed between *mdx* cells transfected with scrambled siRNA (negative control) and *mdx* cardiomyocytes without transfection and kept in culture during 24 h. Therefore the transfection by itself did not interfere with the  $\text{Ca}^{2+}$  signaling response after an osmotic challenge.  $\text{Ca}^{2+}$ -related fluorescence from WT cardiomyocytes ( $F/F_0$ :  $0.98 \pm 0.02$ ) was similar to siRNA treated *mdx* cells ( $F/F_0$ :  $0.94 \pm 0.02$ ). Among several necessary control experiments, we verified successful transfection of siRNA into cardiac myocytes. *Figure 5C* shows cardiomyocytes which were incubated with fluorescently labeled siRNA, to verify siRNA transfection. In addition, siRNA transfection and TRPV2

silencing were validated by Western blot analysis and by quantitative RT-PCR (*Figure 5D*). In siRNA transfected cells, TRPV2 expression was decreased by 60% compared to the negative control (using scrambled siRNA). *Figure 5E* also highlights the integrity of the T-tubular network, as recorded with the fluorescent membrane dye di-8-ANEPPS. Taken together, these data provide strong evidence that siRNA mediated knockdown of TRPV2 normalized the stress-induced  $\text{Ca}^{2+}$  handling in dystrophic cardiomyocytes.

## Discussion

Dystrophin-deficient cardiomyocytes have an abnormally high membrane fragility making them sensitive to mechanical stress.<sup>9</sup> This loss of membrane integrity leads to an increased permeability which allows an abnormal stress-induced influx of extracellular  $\text{Ca}^{2+}$ , presumably via SACs and membrane microruptures.

### The two-hit hypothesis of dystrophic cardiomyopathy

Even though the lack of functional dystrophin protein has been identified as the cause for many forms of this disease, the mechanism(s) linking the absence of this cytoskeletal protein with the observed cellular damage remains poorly understood. Several versions of a “two-hit hypothesis” have been proposed as pathomechanisms of muscular dystrophies and dystrophic cardiomyopathies.<sup>31</sup> These hypotheses postulate a combined effect of abnormal  $\text{Ca}^{2+}$  signals, both from sarcolemmal influx and SR leak, and oxidative stress. In normal muscle, the neuronal nitric oxide synthase (nNOS) is a member of the dystrophin-glycoprotein complex and localized at the sarcolemma. NO can protect cells from stronger oxidative damage by playing an antioxidant role, and by inhibiting NADPH oxidases, the major sources of reactive oxygen species (ROS).<sup>32</sup> In dystrophic myocytes, nNOS is down-regulated contributing to an enhanced generation of ROS.<sup>33</sup> In these cells the abnormal  $\text{Ca}^{2+}$  influx and release further stimulate ROS production by mitochondria and NADPH oxidases, particularly after mechanical stress.<sup>15,34</sup> As a consequence, these ROS may lead to further  $\text{Ca}^{2+}$  influx by increasing the membrane permeability *via* lipid peroxidation and to additional SR release by oxidation of several proteins.<sup>35</sup> Thus, in cardiac muscle, the  $\text{Ca}^{2+}$  signaling pathology defined by the two-hit hypothesis has two components: 1) hypersensitive  $\text{Ca}^{2+}$ -induced  $\text{Ca}^{2+}$  release from the SR (e.g. as sparks or invisible leak), presumably as a result of post-translational modifications of the RyRs (e.g. oxidation, phosphorylation, or hypernitrosylation).<sup>16,36-39</sup> 2) abnormally high  $\text{Ca}^{2+}$  influx across the fragile sarcolemma, particularly after mechanical stress.<sup>5,10,12,40</sup> The relative

importance of these two mechanisms seems to change during the progression of the disease, with the SR leak becoming more and more prominent.<sup>36</sup> Overall, the two-hit mechanism creates an endless loop of abnormal  $\text{Ca}^{2+}$  entry and oxidative damage that may culminate in activation of  $\text{Ca}^{2+}$  dependent proteases and apoptotic or necrotic cell death. In principle, both mechanisms could offer multiple possibilities and targets for future pharmacological treatments.

## **$\text{Ca}^{2+}$ influx via stretch-activated membrane channels**

In the present study we focused on one of the putative pathomechanism involved in abnormal  $\text{Ca}^{2+}$  influx: stretch-activated membrane channels (SACs). The molecular identity of SACs involved in dystrophy is presently unknown. However, previous studies have proposed several candidates as potential SAC subunits in *mdx* cardiomyocytes to explain the elevated  $\text{Ca}^{2+}$  entry during mechanical stress, such as transient receptor potential canonical channel 1 (TRPC1) and 6 (TRPC6).<sup>19,41</sup> Others reported TRPV2 channels to play an important role in dystrophic skeletal muscle fibers.<sup>17,20</sup> Interestingly, overexpression of TRPC3 channels resulted in a dystrophy-like phenotype.<sup>42</sup> Most of these TRP channels form cation channels that are permeable to monovalent and divalent ions, thus carrying entry of both,  $\text{Na}^+$  and  $\text{Ca}^{2+}$ .<sup>43</sup>

## **Identification of TRP channels contributing to SACs**

Unfortunately, the pharmacological tools available to identify particular TRP channels as components of SACs are very unspecific. Most of those compounds affect several or many TRP channels in the same range of concentrations. Therefore, we applied a multipronged approach as the strategy to define the role of TRP channels in the abnormal  $\text{Ca}^{2+}$  signals we observed. Using several available but unspecific pharmacological tools we established a pharmacological profile of the abnormal  $\text{Ca}^{2+}$  signals, as detailed below. This pharmacological profile turned out to be quite unique and suggested that TRPV2 channels might be involved. As a second approach we examined the TRPV2 expression and cellular distribution in normal and dystrophin-deficient cardiomyocytes. These results indicated that TRPV2 channel might indeed play a role in the disease phenotype. Finally, we used more specific tools to pin-point TRPV2 as a component of SACs in dystrophic myocytes. This included the use of blocking antibodies raised against an extracellular epitope of the channels, and the application of siRNA technology to ablate the TRPV2 protein.

## TRPV2 protein is overexpressed in dystrophic cardiomyocytes

Histologically, TRPV2 proteins have been identified in various tissues and organs such as brain, lungs, skeletal and cardiac muscle.<sup>44</sup> Their function is not yet well elucidated, but previous studies highlighted their involvement in sensation of excessive heat, osmosensory mechanisms, insulin exocytosis and cardiovascular functions.<sup>7,27,45,46</sup> Under physiological conditions, immunoelectron microscopy studies revealed a TRPV2 localization in intracellular membrane compartments, specifically in the endoplasmic reticulum. Nevertheless, upon specific stimulation, TRPV2 proteins are translocated to the sarcolemma to mediate an extracellular  $\text{Ca}^{2+}$  influx.<sup>47</sup> It has been proposed that the translocation of TRPV2 could resemble that of glucose transporter 4 (GLUT4). GLUT4 is an insulin-regulated glucose transporter translocated from an intracellular storage to the plasma membrane upon insulin stimulation in adipocytes and in skeletal muscle fibers. Upon insulin growth factor-1 (IGF-1) stimulation, TRPV2 channels are targeted to the sarcolemma *via* the phosphatidylinositol 3-kinase (PI3K) pathways.<sup>46,48</sup> Recently, new insight about this cation channels has been obtained in several pathological conditions. In dystrophic skeletal muscle fibers and myotubes in culture, TRPV2 channels were observed to be translocated from the intracellular space to the sarcolemma.<sup>17,20,49,50</sup> In agreement with these observations, in our study, *mdx* cardiomyocytes displayed a strong TRPV2 localization at the sarcolemma and along the T-tubular network, when compared to WT cells. Moreover, we found that this abnormal translocation is accompanied by a TRPV2 overexpression, particularly at the sarcolemma, as suggested by biotinylation assays. Together, the elevated expression and translocation of TRPV2 channels in dystrophic cardiomyocytes are clearly consistent with their possible role in SACs and, further, suggest a stronger activity of TRPV2 in these cells.

## TRPV2 as potential components of SACs is supported by unspecific TRP channel pharmacology

To assess the TRPV2 function at the plasma membrane of dystrophic myocytes, a pharmacological approach was used. As mentioned above, a known problem in the field of TRP channel research is the lack of highly specific pharmacological tools.<sup>51</sup> Furthermore, the efficiency of many compounds depends on the cell type and even the species.<sup>47</sup> In many cases, several unspecific compounds are used experimentally to block various TRP channels, such as ruthenium red, 2-APB, and SKF96365. For few channels some specific agonists are available, such as capsaicin for TRPV1 channels. Another promising strategy is to apply a compound that activates some TRP channels but blocks others. 2-APB, which is a blocker of many TRP

channels, was the first activator identified for some TRPV channels, including TRPV2, in HEK293 cells.<sup>47</sup> Indeed, in our experiments with cardiomyocytes pretreated with thapsigargin and ryanodine (to eliminate SR function), the application of 2-APB elicited Ca<sup>2+</sup> influx from the extracellular space, that could be inhibited with ruthenium red. Consistent with a role of TRPV2 in Ca<sup>2+</sup> influx, the blocker SKF96365 also suppressed the stress induced Ca<sup>2+</sup> signals.<sup>26</sup> There are two pharmacological TRPV2 modulators, probenecid and tranilast (activator and inhibitor, respectively) that have been reported to exhibit somewhat better specificity for TRPV2 channels. Probenecid was initially synthesized to reduce the renal excretion of antibiotics, particularly penicillin, and recently it has been identified as an agonist of TRPV2.<sup>52,53</sup> Tranilast is clinically used as an antiallergic drug and experimentally as a TRPV2 antagonist.<sup>46</sup> Both compounds changed Ca<sup>2+</sup> influx in dystrophic myocytes with eliminated SR function in a way that was perfectly consistent with TRPV2 underlying this kind of influx. In summary, the analysis of the pharmacological profile revealed by our experiments allowed us to consider a pathological TRPV2 function in *mdx* cardiomyocytes.

## **Specific inhibition of TRPV2 protects dystrophic myocytes from abnormal Ca<sup>2+</sup> signals**

To specifically probe whether TRPV2 channels are responsible for the Ca<sup>2+</sup> increase after an osmotic shock in dystrophic myocytes, we applied an antibody raised against an extracellular epitope of the channel. If the channel pores are indeed blocked by these antibodies, this strategy suppresses the TRPV2 protein function and Ca<sup>2+</sup> can no longer enter the cytoplasm. However, the specificity of blocking antibodies has been challenged in different studies and may depend on a variety of parameters such as the type of experiments (Western blot, immunocytochemistry), species (rat, mouse), type of antibodies (polyclonal, monoclonal). Therefore, we carried out several control experiments using other antibodies during the osmotic stress. As negative control experiments, we used antibodies raised against an intracellular epitope of the TRPV2 channel and against an extracellular epitope of TRPC1. In these experiments, we did not observe any inhibition of the TRPV2 function since the Ca<sup>2+</sup>-related fluorescence in *mdx* cells increased in the same manner as without antibodies. Therefore, we concluded that incubation with a TRPV2 antibody against an extracellular epitope eliminated the stress-induced signals by specifically blocking TRPV2.

Another approach to specifically interfere with the function of the channel is the use of small interfering RNA (siRNA) against TRPV2 mRNA. After entering the cell by transfection, this specific siRNA binds the TRPV2 mRNA by complementarity. This binding prevents the



TRPV2 mRNA translation after transcription by specific destruction of the mRNA by exonucleases, essentially preventing the protein synthesis. After incubation of *mdx* myocytes with siRNA, Western blot and quantitative RT-PCR experiments confirmed the decrease of the expression of TRPV2 protein (down to 40 % ) compared to dystrophic cells transfected with scrambled siRNA. Myocytes were maintained in short-term primary culture for 24 h before carrying out the experiments to allow for the normal degradation of pre-existing TRPV2 protein. The results showed that the Ca<sup>2+</sup>-related fluorescence after an osmotic challenge in *mdx* myocytes transfected with anti-TRPV2 siRNA was comparable to WT cells, while *mdx* myocytes transfected with scrambled siRNA behaved like untransfected dystrophic cells.

## Conclusion

Taken together, our observations indicate a major role of TRPV2 channels in the cardiac dystrophic Ca<sup>2+</sup> signaling pathology and provide compelling evidence that the TRPV2 proteins form a subunit of stretch activated channels.

## TRPV2 channels and dystrophinopathies

Dystrophinopathies give rise to a wide spectrum of muscle diseases. Most forms include cardiac muscle participation. The most severe is DMD, characterized by the absence of dystrophin. Becker muscular dystrophy (BMD) results in a milder phenotype since dystrophin is produced but only partly functional. In X-linked cardiomyopathy (XLDCM), dystrophin is absent only in the cardiac muscle. These three dystrophinopathies all progress into a dilated cardiomyopathy.<sup>54</sup> As mentioned above, the two-hit hypothesis postulates a major pathological role for abnormal Ca<sup>2+</sup> influx across the sarcolemma as one of the main pathomechanisms. Our study reveals that TRPV2 proteins are abnormally recruited and activated in dystrophic cardiac myocytes. Thus, the TRPV2 proteins, their function and translocation pathway could be relevant targets for future pharmacological treatments of these and related pathologies.

## Funding

Swiss National Science Foundation (31-132689 and 31-156375 to E.N.), the Swiss Foundation for Research on Muscle Diseases and the National Center of Competences in Research (NCCR “TransCure”).

## **Acknowledgements**

We would like to thank G. Rigoli, S. Schneider and M. Courtehoux for expert technical help.

## **Conflict of Interest**

Conflict of Interest: none declared



## References

1. Ferlini A, Sewry C, Melis MA, Mateddu A, Muntoni F. X-linked dilated cardiomyopathy and the dystrophin gene. *Neuromuscular Disord.* 1999;**9**:339–346.
2. Monaco AP, Neve RL, Colletti-Feener C, Bertelson CJ, Kurnit DM, Kunkel LM. Isolation of candidate cDNAs for portions of the Duchenne muscular dystrophy gene. *Nature.* 1986;**323**:646–650.
3. Lorin C, Gueffier M, Bois P, Faivre JF, Cognard C, Sebille S. Ultrastructural and functional alterations of EC coupling elements in *mdx* cardiomyocytes: an analysis from membrane surface to depth. *Cell Biochem Biophys.* 2013;**66**:723–736.
4. Ervasti JM, Campbell KP. A role for the dystrophin-glycoprotein complex as a transmembrane linker between laminin and actin. *J Cell Biol.* 1993;**122**:809–823.
5. Petrof BJ, Shrager JB, Stedman HH, Kelly AM, Sweeney HL. Dystrophin protects the sarcolemma from stresses developed during muscle contraction. *PNAS.* 1993;**90**:3710–3714.
6. Vandebrouck C. Involvement of TRPC in the abnormal calcium influx observed in dystrophic (*mdx*) mouse skeletal muscle fibers. *J Cell Biol.* 2002;**158**:1089–1096.
7. Iwata Y. A novel mechanism of myocyte degeneration involving the Ca<sup>2+</sup>-permeable growth factor-regulated channel. *J Cell Biol.* 2003;**161**:957–967.
8. Leijendekker WJ, Passaquin AC, Metzinger L, Rüegg UT. Regulation of cytosolic calcium in skeletal muscle cells of the *mdx* mouse under conditions of stress. *Br J Pharmacol.* 1996;**118**:611–616.
9. Yasuda S, Townsend D, Michele DE, Favre EG, Day SM, Metzger JM. Dystrophic heart failure blocked by membrane sealant poloxamer. *Nature.* 2005;**436**:1025–1029.
10. Allen DG, Whitehead NP. Duchenne muscular dystrophy--what causes the increased membrane permeability in skeletal muscle? *Int J Biochem Cell Biol.* 2011;**43**:290–294.
11. Sachs F. Stretch-activated ion channels: what are they? *Physiology (Bethesda).* 2010;**25**:50–56.

12. Fanchaouy M, Polakova E, Jung C, Ogrodnik J, Shirokova N, Niggli E. Pathways of abnormal stress-induced  $\text{Ca}^{2+}$  influx into dystrophic *mdx* cardiomyocytes. *Cell Calcium*. 2009;**46**:114–121.
13. Williams IA, Allen DG. Intracellular calcium handling in ventricular myocytes from *mdx* mice. *Am J Physiol Heart Circ Physiol*. 2006;**292**:H846–H855.
14. Matsumura CY, Taniguti APT, Pertille A, Neto HS, Marques MJ. Stretch-activated calcium channel protein TRPC1 is correlated with the different degrees of the dystrophic phenotype in *mdx* mice. *Am J Physiol Cell Physiol*. 2011;**301**:C1344–C1350.
15. Jung C, Martins AS, Niggli E, Shirokova N. Dystrophic cardiomyopathy: amplification of cellular damage by  $\text{Ca}^{2+}$  signalling and reactive oxygen species-generating pathways. *Cardiovasc Res*. 2008;**77**:766–773.
16. Ullrich ND, Fanchaouy M, Gusev K, Shirokova N, Niggli E. Hypersensitivity of excitation-contraction coupling in dystrophic cardiomyocytes. *Am J Physiol Heart Circ Physiol*. 2009;**297**:H1992–H2003.
17. Zanou N, Iwata Y, Schakman O, Lebacqz J, Wakabayashi S, Gailly P. Essential role of TRPV2 ion channel in the sensitivity of dystrophic muscle to eccentric contractions. *FEBS Lett*. 2009;**583**:3600–3604.
18. Díaz ME, Graham HK, O’Neill SC, Trafford AW, Eisner DA. The control of sarcoplasmic reticulum Ca content in cardiac muscle. *Cell Calcium*. 2005;**38**:391–396.
19. Ward ML, Williams IA, Chu Y, Cooper PJ, Ju YK, Allen DG. Stretch-activated channels in the heart: Contributions to length-dependence and to cardiomyopathy. *Prog Biophys Mol Biol*. 2008;**97**:232–249.
20. Harisseh R, Chatelier A, Magaud C, Deliot N, Constantin B. Involvement of TRPV2 and SOCE in calcium influx disorder in DMD primary human myotubes with a specific contribution of  $\alpha$ 1-syntrophin and PLC/PKC in SOCE regulation. *Am J Physiol Cell Physiol*. 2013;**304**:C881–C894.
21. Rubinstein J, Lasko VM, Koch SE, Singh VP, Carreira V, Robbins N, Patel AR, Jiang M, Bidwell P, Kranias EG, Jones WK, Lorenz JN. Novel role of transient receptor potential vanilloid 2 in the regulation of cardiac performance. *Am J Physiol Heart Circ Physiol*. 2014;**306**:H574–H584.

22. Katanosaka Y, Iwasaki K, Ujihara Y, Takatsu S, Nishitsuji K, Kanagawa M, Sudo A, Toda T, Katanosaka K, Mohri S, Naruse K. TRPV2 is critical for the maintenance of cardiac structure and function in mice. *Nat Commun.* 2014;**5**:3932.
23. Frank JS, Mottino G, Reid D, Molday RS, Philipson KD. Distribution of the Na<sup>+</sup>-Ca<sup>2+</sup> exchange protein in mammalian cardiac myocytes: an immunofluorescence and immunocolloidal gold-labeling study. *J Cell Biol.* 1992;**117**:337–345.
24. Koch SE, Gao X, Haar L, Jiang M, Lasko VM, Robbins N, Cai W, Brokamp C, Varma P, Tranter M, Liu Y, Ren X, Lorenz JN, Wang H-S, Jones WK, Rubinstein J. Probenecid: Novel use as a non-injurious positive inotrope acting via cardiac TRPV2 stimulation. *J Mol Cell Cardiol.* 2012;**53**:134–144.
25. Swiderski K, Todorov M, Gehrig SM, Naim T, Chee A, Stapleton DI, Koopman R, Lynch GS. Tranilast administration reduces fibrosis and improves fatigue resistance in muscles of mdx dystrophic mice. *Fibrogenesis Tissue Repair.* 2014;**7**:1.
26. Juvin V, Penna A, Chemin J, Lin Y-L, Rassendren F-A. Pharmacological characterization and molecular determinants of the activation of transient receptor potential V2 channel orthologs by 2-aminoethoxydiphenyl borate. *Molecular Pharmacol.* 2007;**72**:1258–1268.
27. Muraki K, Iwata Y, Katanosaka Y, Ito T, Ohya S, Shigekawa M, Imaizumi Y. TRPV2 is a component of osmotically sensitive cation channels in murine aortic myocytes. *Circ Res.* 2003;**93**:829–838.
28. Ng LC, O'Neill KG, French D, Airey JA, Singer CA, Tian H, Shen XM, Hume JR. TRPC1 and Orai1 interact with STIM1 and mediate capacitative Ca<sup>2+</sup> entry caused by acute hypoxia in mouse pulmonary arterial smooth muscle cells. *AJP: Cell Physiology.* 2012;**303**:C1156–C1172.
29. Tian Q, Pahlavan S, Oleinikow K, Jung J, Ruppenthal S, Scholz A, Schumann C, Kraegeloh A, Oberhofer M, Lipp P, Kaestner L. Functional and morphological preservation of adult ventricular myocytes in culture by sub-micromolar cytochalasin D supplement. *J Mol Cell Cardiol.* 2012;**52**:113–124.
30. Ramabadran RS, Chancey A, Vallejo JG, Barger PM, Sivasubramanian N, Mann DL. Targeted gene silencing of tumor necrosis factor attenuates the negative inotropic effects of

lipopolysaccharide in isolated contracting cardiac myocytes. *Tex Heart Inst J*. 2008;**35**:16–21.

31. Rando TA. Role of nitric oxide in the pathogenesis of muscular dystrophies: a ‘two hit’ hypothesis of the cause of muscle necrosis. *Microsc Res Tech*. 2001;**55**:223–235.
32. Zhang Y, Tocchetti CG, Krieg T, Moens AL. Oxidative and nitrosative stress in the maintenance of myocardial function. *Free Radic Biol Med*. 2012;**53**:1531–1540.
33. Bia BL, Cassidy PJ, Young ME, Rafael JA, Leighton B, Davies KE, Radda GK, Clarke K. Decreased myocardial nNOS, increased iNOS and abnormal ECGs in mouse models of Duchenne muscular dystrophy. *J Mol Cell Cardiol*. 1999;**31**:1857–1862.
34. Prosser BL, Ward CW, Lederer WJ. X-ROS Signaling: Rapid mechano-chemo transduction in heart. *Science*. 2011;**333**:1440–1445.
35. Vandebrouck A, Sabourin J, Rivet J, Balghi H, Seville S, Kitzis A, Raymond G, Cognard C, Bourmeyster N, Constantin B. Regulation of capacitative calcium entries by  $\beta$ 1-syntrophin: association of TRPC1 with dystrophin complex and the PDZ domain of  $\beta$ 1-syntrophin. *FASEB J*. 2007;**21**:608–617.
36. Kyrychenko S, Poláková E, Kang C, Pocsai K, Ullrich ND, Niggli E, Shirokova N. Hierarchical accumulation of RyR post-translational modifications drives disease progression in dystrophic cardiomyopathy. *Cardiovasc Res*. 2013;**97**:666–675.
37. Sarma S, Li N, van Oort RJ, Reynolds C, Skapura DG, Wehrens XHT. Genetic inhibition of PKA phosphorylation of RyR2 prevents dystrophic cardiomyopathy. *PNAS*. 2010;**107**:13165–13170.
38. Fauconnier J, Thireau J, Reiken S, Cassan C, Richard S, Matecki S, Marks AR, Lacampagne A. Leaky RyR2 trigger ventricular arrhythmias in Duchenne muscular dystrophy. *PNAS*. 2010;**107**:1559–1564.
39. Bellinger AM, Reiken S, Carlson C, Mongillo M, Liu X, Rothman L, Matecki S, Lacampagne A, Marks AR. Hypernitrosylated ryanodine receptor calcium release channels are leaky in dystrophic muscle. *Nat Med*. 2009;**15**:325–330.
40. Allen DG, Gervasio OL, Yeung EW, Whitehead NP. Calcium and the damage pathways in muscular dystrophy. *Can J Physiol Pharmacol*. 2010;**88**:83–91.

41. Dyachenko V, Husse B, Rueckschloss U, Isenberg G. Mechanical deformation of ventricular myocytes modulates both TRPC6 and Kir2.3 channels. *Cell Calcium*. 2009;**45**:38–54.
42. Millay DP, Goonasekera SA, Sargent MA, Maillet M, Aronow BJ, Molkentin JD. Calcium influx is sufficient to induce muscular dystrophy through a TRPC-dependent mechanism. *PNAS*. 2009;**106**:19023–19028.
43. Owsianik G, Talavera K, Voets T, Nilius B. Permeation and selectivity of TRP channels. *Annu Rev Physiol*. 2006;**68**:685–717.
44. Kowase T, Nakazato Y, Yoko-O H, Morikawa A, Kojima I. Immunohistochemical localization of growth factor-regulated channel (GRC) in human tissues. *Endocr J*. 2002;**49**:349–355.
45. Caterina MJ, Rosen TA, Tominaga M, Brake AJ, Julius D. A capsaicin-receptor homologue with a high threshold for noxious heat. *Nature*. 1999;**398**:436–441.
46. Aoyagi K, Ohara Imaizumi M, Nishiwaki C, Nakamichi Y, Nagamatsu S. Insulin/phosphoinositide 3-kinase pathway accelerates the glucose-induced first-phase insulin secretion through TrpV2 recruitment in pancreatic  $\beta$ -cells. *Biochem J*. 2010;**432**:375–386.
47. Perálvarez-Marín A, Doñate-Macian P, Gaudet R. What do we know about the transient receptor potential vanilloid 2 (TRPV2) ion channel? *FEBS J*. 2013;**280**:5471–5487.
48. Dogra C, Changotra H, Wergedal JE, Kumar A. Regulation of phosphatidylinositol 3-kinase (PI3K)/Akt and nuclear factor-kappa B signaling pathways in dystrophin-deficient skeletal muscle in response to mechanical stretch. *J Cell Physiol*. 2006;**208**:575–585.
49. Iwata Y, Katanosaka Y, Arai Y, Shigekawa M, Wakabayashi S. Dominant-negative inhibition of  $\text{Ca}^{2+}$  influx via TRPV2 ameliorates muscular dystrophy in animal models. *Hum Mol Gen*. 2009;**18**:824–834.
50. Iwata Y, Ohtake H, Suzuki O, Matsuda J, Komamura K, Wakabayashi S. Blockade of sarcolemmal TRPV2 accumulation inhibits progression of dilated cardiomyopathy. *Cardiovasc Res*. 2013;**99**:760–768.

51. Wu L-J, Sweet T-B, Clapham DE. International Union of Basic and Clinical Pharmacology. LXXVI. Current progress in the mammalian TRP ion channel family. *Pharmacol Rev.* 2010;**62**:381–404.
52. Vriens J, Appendino G, Nilius B. Pharmacology of vanilloid transient receptor potential cation channels. *Molecular Pharmacol.* 2009;**75**:1262–1279.
53. Hill G, Cihlar T, Oo C, Ho ES, Prior K, Wiltshire H, Barrett J, Liu B, Ward P. The anti-influenza drug oseltamivir exhibits low potential to induce pharmacokinetic drug interactions via renal secretion-correlation of in vivo and in vitro studies. *Drug Metab Dispos.* 2002;**30**:13–19.
54. Morrison LA. Dystrophinopathies. *Handb Clin Neurol.* 2011;**101**:11–39.

## Figure legends:

**Figure 1** Stress-induced intracellular  $\text{Ca}^{2+}$  signals in *mdx* and wild-type (WT) mouse ventricular cardiomyocytes. (A) Images of  $\text{Ca}^{2+}$ -related fluo-3 fluorescence obtained in WT (top) and *mdx* cardiomyocytes (bottom) at the indicated times before (10 s) during (50 s) and after the osmotic stress (80 s and 200 s). Note the more pronounced  $\text{Ca}^{2+}$  signals in *mdx* myocytes. (B) Time course of normalized and averaged  $\text{Ca}^{2+}$ -related fluorescence, pooled from *mdx* (black circles) and WT (grey circles) cardiomyocytes undergoing the osmotic stress protocol. The lines on the top represent the protocol by which extracellular solutions were changed. (C) Left, mean values of normalized fluorescence during 40 s after the osmotic shock. Right, estimates of SR  $\text{Ca}^{2+}$  content by 10 mM caffeine stimulation before and after the osmotic challenge. n=10-17 cells from N=2 mice for WT; and n=13-14 from N=2-4 for *mdx*. \*  $P < 0.05$ , \*\*  $P < 0.01$ , ns: not significant.

**Figure 2** Subcellular TRPV2 localization and expression in *mdx* cardiomyocytes. (A) Immunostaining against an extracellular epitope of TRPV2 (green) and NCX (red) in WT (above) and *mdx* (below) cardiomyocytes. (B) Western blot analysis of normalized TRPV2 channels and  $\beta$ -actin expression in cardiac myocytes. Blot was cut to reduce a wide gap between neighboring lanes and bands. (C) Sarcolemma specific TRPV2, GAPDH (control), and P44/P42 MAPK (negative control) expressions (quantified by Western blot after biotinylation). P44/P42 MAPK and GAPDH signals were obtained by reprobng after stripping, the TRPV2 band is contrast enhanced. Cardiomyocytes were isolated from N=4-7 *mdx* and WT mice. \*  $P < 0.05$ , \*\*  $P < 0.01$ .

**Figure 3** Pharmacology of transient receptor potential vanilloid type 2 (TRPV2) channels. (A) Left, time courses of cytosolic  $\text{Ca}^{2+}$  in *mdx* cardiomyocytes during application of the TRPV2 activator 2-APB (500  $\mu\text{M}$ , at the arrow), with or without the TRPV2 inhibitor ruthenium red (RuR, 40  $\mu\text{M}$ ). Cells were pretreated with thapsigargin (Tg, 1  $\mu\text{M}$ ), ryanodine (Rya, 10  $\mu\text{M}$ ) and caffeine puffs (Caff, 10 mM) to suppress SR function. Right, mean values of normalized  $\text{Ca}^{2+}$  related fluorescence averaged between 90 and 100 s. (B) Left, time courses of cytosolic  $\text{Ca}^{2+}$  in *mdx* myocytes with abolished SR, then perfused (arrow) with the TRPV2 activator probenecid (Pro, 1 mM), with or without the TRPV2 inhibitor tranilast (Tran, 1 mM). Right, mean values of normalized  $\text{Ca}^{2+}$ -related fluorescence averaged during 20 s at the end of the recording. (C) and (D) Left, time courses of normalized average fluorescence pooled from in *mdx* (black circles, C and D), WT (dark grey circles, C), *mdx* cardiomyocytes perfused with the inhibitors SKF 96365

(30  $\mu$ M; light grey circles, *C*), RuR (40  $\mu$ M; light grey circles, *D*), and Tran (1 mM; dark grey circles, *D*). The lines on the top represent the protocol by which extracellular solutions were changed. Time courses of WT and *mdx* myocytes are replotted from Figure 1 for easier comparison with the trace obtained from dystrophic cells in the presence of SKF 96365, RuR and Tran. (*C*) and (*D*) Right, mean values of normalized fluorescence during 40 s after the osmotic shock.  $n = 8-25$ ,  $N=2$  for each experiment. \*\*  $P < 0.01$ .

**Figure 4** Stress-induced intracellular  $Ca^{2+}$  signals reduced by TRPV2 antibody in *mdx* ventricular cardiomyocytes. (*A*) Time courses of normalized  $Ca^{2+}$ -related fluorescence pooled from *mdx* cardiomyocytes pretreated (grey circles) or not (black circles) with an antibody against an extracellular epitope of TRPV2 (Alomone ACC-39). The lines on the top represent the protocol by which extracellular solutions were changed. (*B*) Mean values of normalized fluorescence during 40 s following the osmotic shock in blocking antibodies against an extracellular epitope of TRPV2 and negative control antibodies (against an intracellular epitope of TRPV2 and against an extracellular epitope of TRPC1). (*C*) Estimates of SR  $Ca^{2+}$  content by 10 mM caffeine stimulation. Each experiment  $n=4-9$  and  $N=2$ . \*\*  $P < 0.01$ , ns: not significant.

**Figure 5** siRNA ablation of TRPV2 in *mdx* cardiomyocytes. (*A*) Time courses of normalized  $Ca^{2+}$  related fluorescence pooled from *mdx* myocytes transfected with siRNA directed against TRPV2 (grey circles) or scrambled siRNA as a negative control (black circles). Line on the top represents the protocol by which extracellular solutions were changed. (*B*) Mean values of normalized fluorescence during 40 s after the osmotic shock obtained from untransfected *mdx* myocytes, *mdx* cells transfected with scrambled siRNA, *mdx* cells transfected with siRNA against TRPV2 and WT cardiomyocytes. WT data replotted for comparison. (*C*) Fluorescence and transmission images of *mdx* ventricular cardiomyocytes showing successful transfection with fluorescently labelled siRNA. (*D*) Statistical analysis of reduced protein and messenger RNA expressions by Western blot (left and inset) and by RT-PCR (right) in *mdx* cardiomyocytes after transfection with siRNA directed against TRPV2. (*E*) Confocal images of T-tubular network with di-8ANEPPS membrane staining after transfection with scrambled siRNA and siRNA against TRPV2, respectively.  $n=7-11$ ,  $N=4-8$ . \*  $P < 0.05$ , \*\*  $P < 0.01$ , ns: not significant.



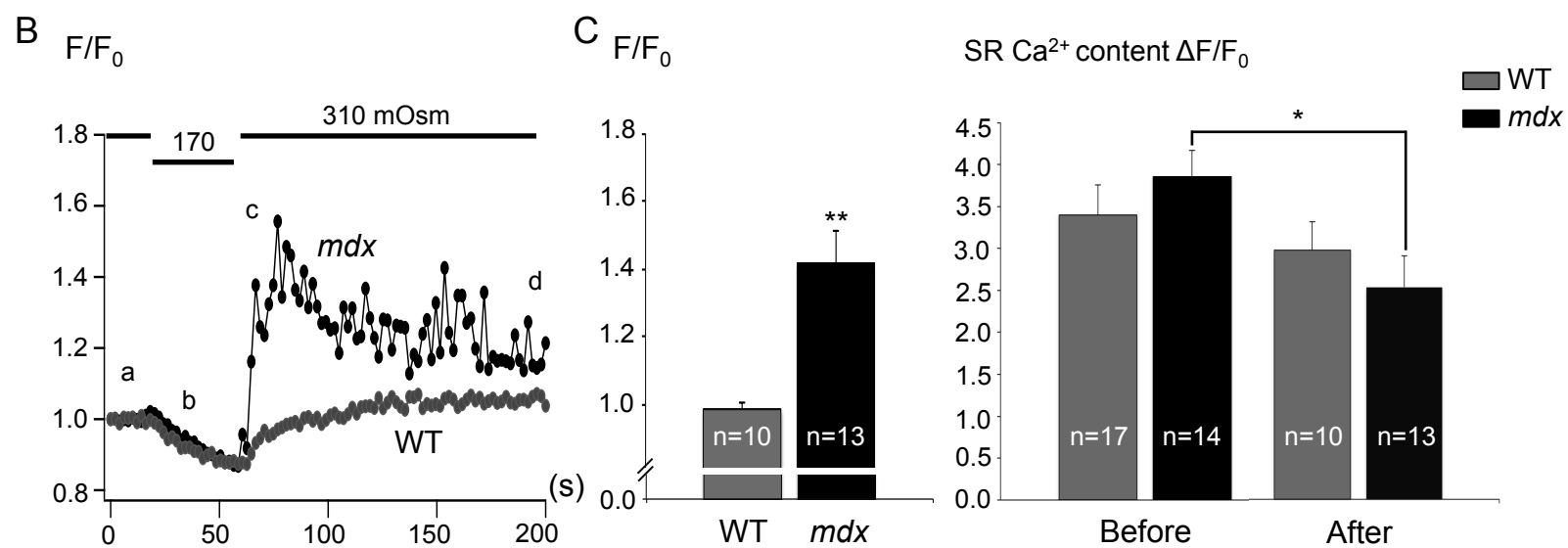
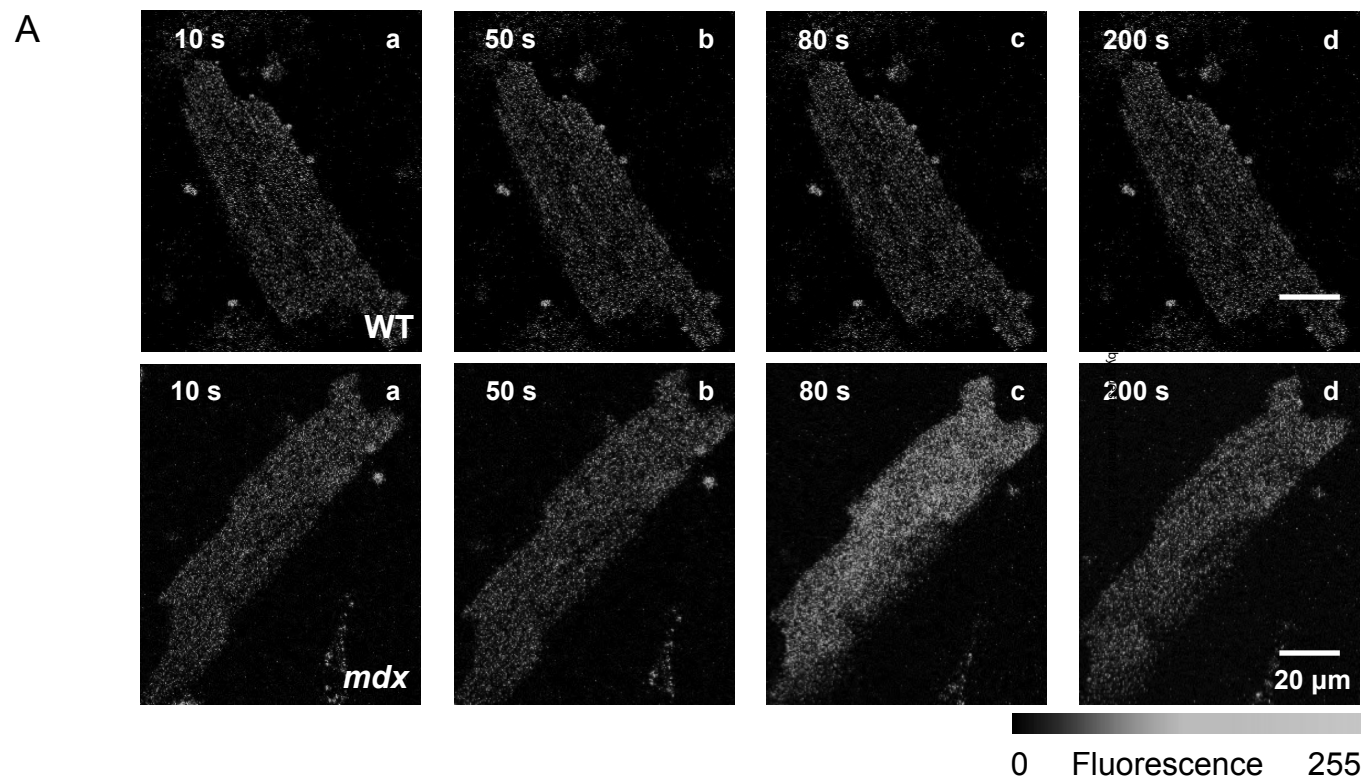


Figure 1

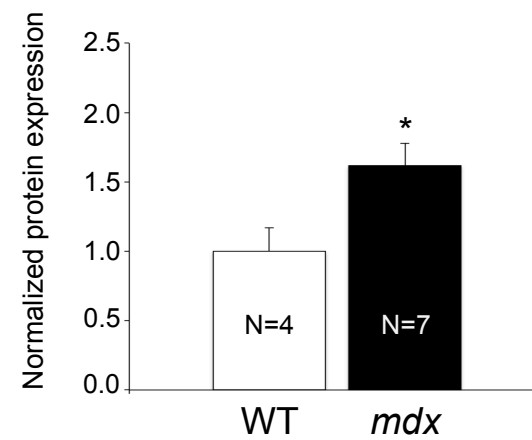
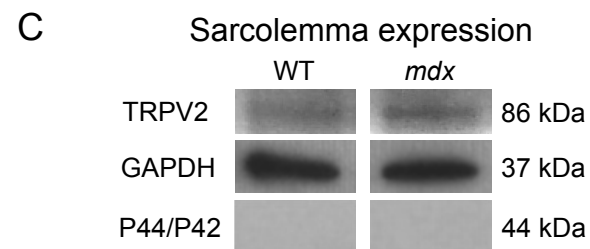
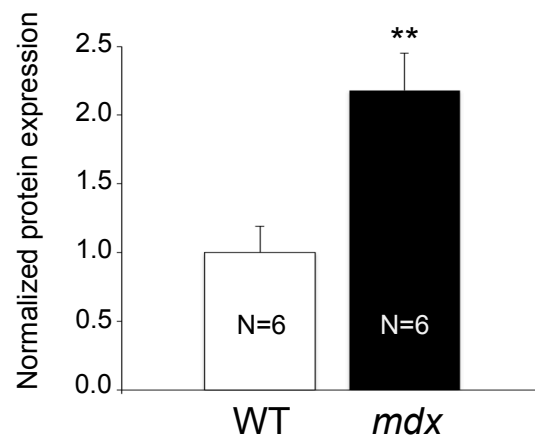
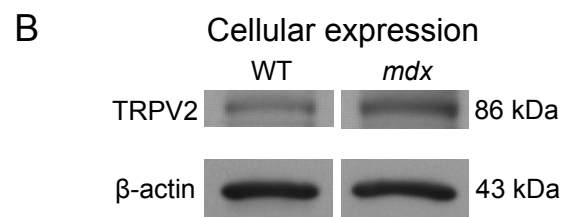
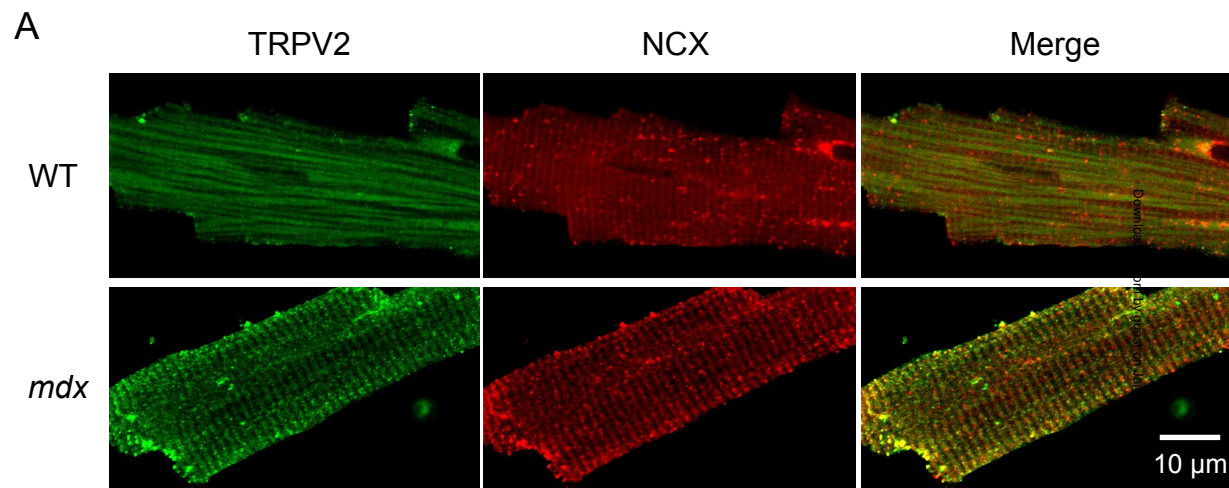


Figure 2

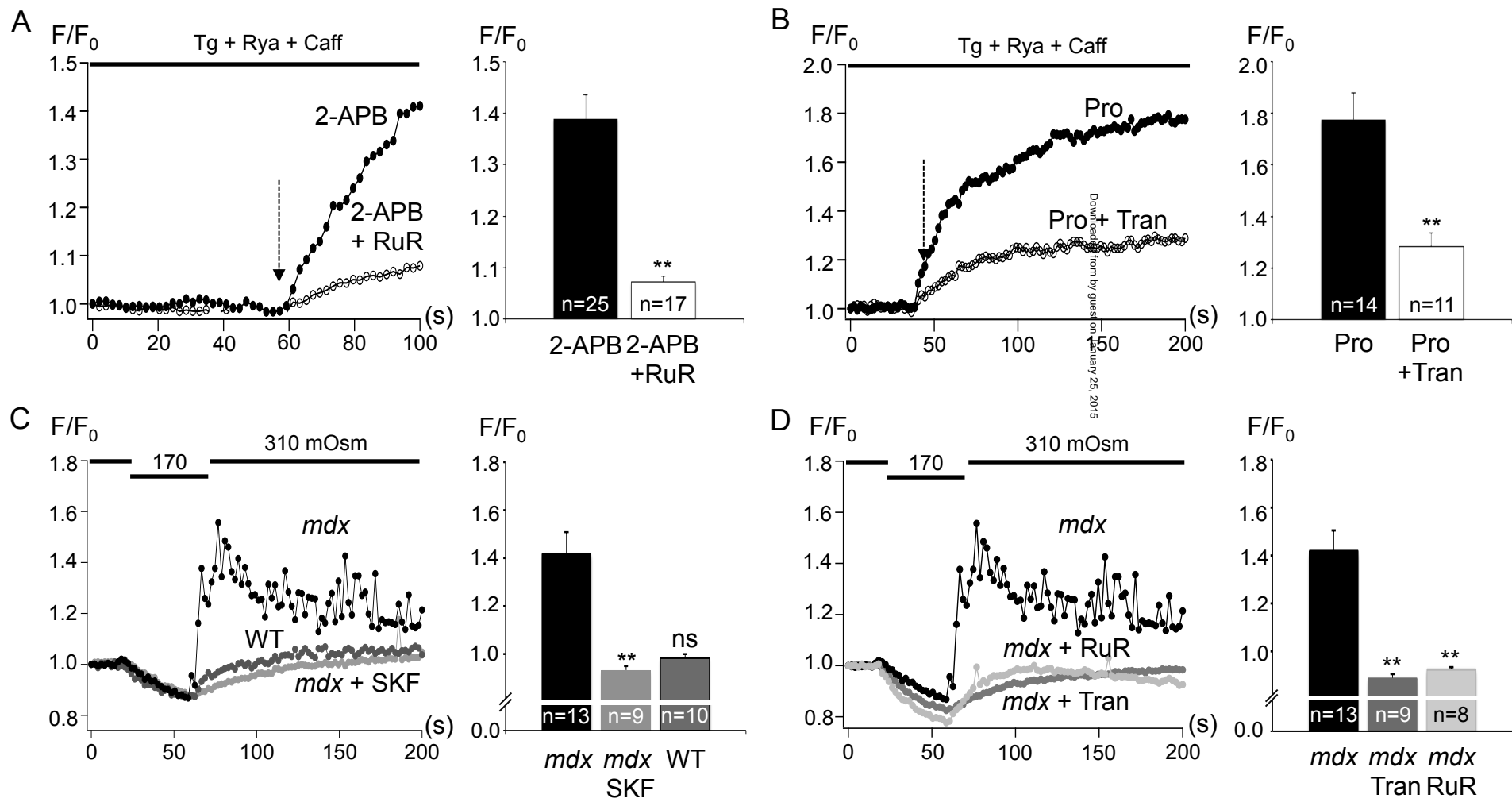


Figure 3

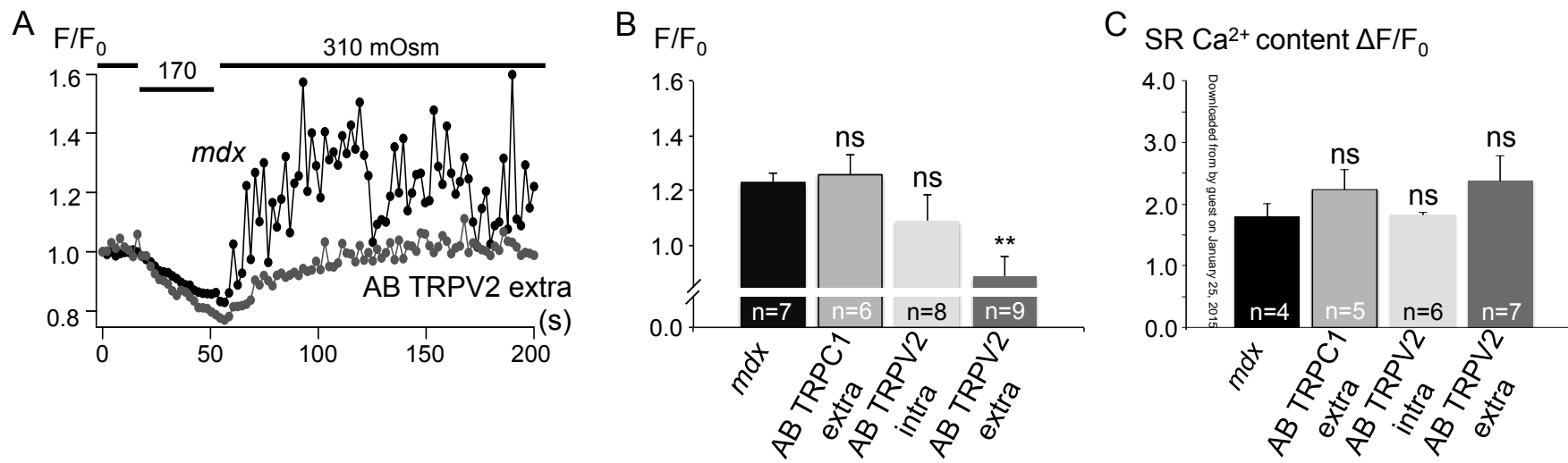


Figure 4

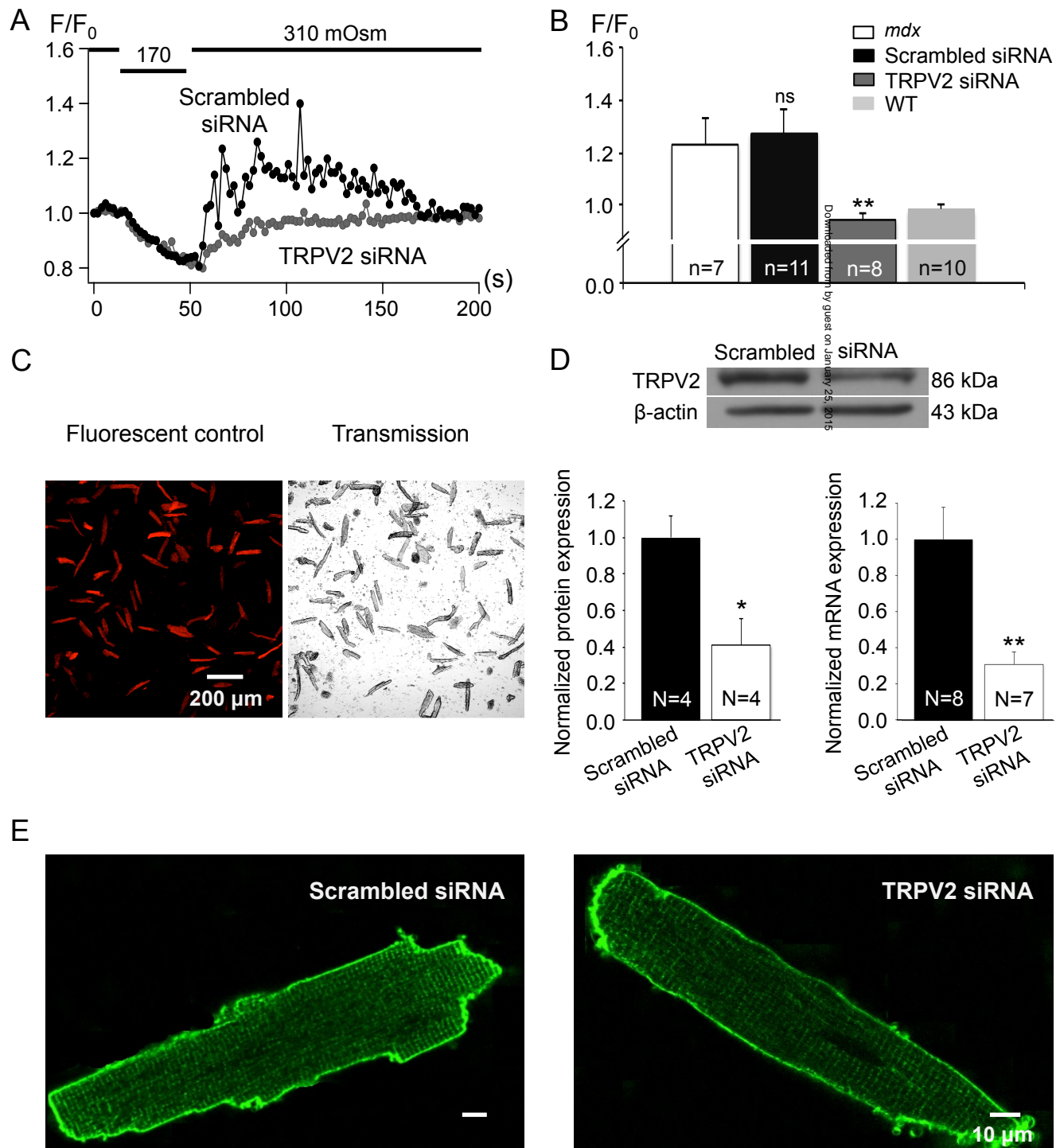


Figure 5